frontiers | Frontiers in Nutrition

ORIGINAL RESEARCH
published: 16 May 2022
doi: 10.3389/fnut.2022.876992

Structural Characterization of *Gracilariopsis lemaneiformis* Polysaccharide and Its Property in Delaying Cellular Senescence

Xiaomei Wang[1†], *Xiaogang Xu*[2†], *Genxiang Mao*[2*], *Yue Guo*[1], *Guangce Wang*[3], *Xue Sun*[4], *Nianjun Xu*[4*] and *Zhongshan Zhang*[1*]

[1] *Key Laboratory of Vector Biology and Pathogen Control of Zhejiang Province, Huzhou University, Huzhou, China,* [2] *Key Lab of Geriatrics & Geriatrics Institute of Zhejiang Province, Department of Geriatrics, Zhejiang Hospital, Hangzhou, China,* [3] *CAS and Shandong Province Key Laboratory of Experimental Marine Biology, Center for Ocean Mega-Science, Institute of Oceanology, Chinese Academy of Sciences, Qingdao, China,* [4] *National Engineering Research Laboratory of Marine Biotechnology and Engineering, Key Laboratory of Aquacultural Biotechnology, Ministry of Education, Collaborative Innovation Center for Zhejiang Marine High-Efficiency and Healthy Aquaculture, Key Laboratory of Marine Biotechnology of Zhejiang Province, Ningbo University, Ningbo, China*

The sulfated polysaccharide was isolated from the purified *G. lemaneiformis* polysaccharide (PGP), and its property in delaying H_2O_2-induced 2BS cellular senescence was studied. The results showed that PGP was a linear polysaccharide containing alternating α-(1→ 3)- and β-(1→ 4)-galactopyranose units. Most of the sulfate groups are at C6 of the -(1→ 4)-α-D-Galp, and a small part of them are at C3 and C6. PGP pretreatment could decrease SA-β-gal-positive cells and prevent the formation of senescence-associated heterochromatic foci (SAHF) induced by H_2O_2 in a dose-dependent manner. It is speculated that PGP may delay aging by downregulating the expression of p21 and p53 genes. The finding provides new insights into the beneficial role of *G. lemaneiformis* polysaccharide (GP) on retarding senescence process.

Keywords: *G. lemaneiformis*, polysaccharide, cellular senescence, SA-β-gal, p53-p21 pathway

OPEN ACCESS

Edited by:
Shuai Chen,
Wuhan University, China

Reviewed by:
Bo Jin,
Zhejiang Chinese Medical University, China
Zhipeng Tao,
Massachusetts General Hospital and Harvard Medical School, United States

***Correspondence:**
Zhongshan Zhang
01959@zjhu.edu.cn
Genxiang Mao
maogenxiang@163.com
Nianjun Xu
xunianjun@nbu.edu.cn

[†] *These authors have contributed equally to this work and share first authorship*

Specialty section:
This article was submitted to Food Chemistry, a section of the journal Frontiers in Nutrition

Received: *16 February 2022*
Accepted: *19 April 2022*
Published: *16 May 2022*

Citation:
Wang X, Xu X, Mao G, Guo Y, Wang G, Sun X, Xu N and Zhang Z (2022) Structural Characterization of Gracilariopsis lemaneiformis Polysaccharide and Its Property in Delaying Cellular Senescence. Front. Nutr. 9:876992. doi: 10.3389/fnut.2022.876992

INTRODUCTION

Cellular senescence is a physiological stress response of mammalian cells which results in the development of senescent cells with distinct physical, molecular, and metabolic signatures (1). In fact, aging is a key cellular program that can be induced and plays an important role in permanently limiting the reproduction of damaged and defective cells (2). Human embryonic fibroblasts can be cultured *in vitro* for about 50 generations. With the increase of generations, cell division and proliferation are slow and gradually show the characteristics of cell aging. The main result is that the cell volume increases, cell heterogeneity increases, and chromosome aberration and lysosome increase (3). Growth arrest is not only a prominent manifestation of cell aging but also an important factor causing biological aging. Therefore, the aging response can be prematurely induced in cells through the application of endogenous and exogenous stimuli *in vitro* and *in vivo*. H_2O_2 has been the most commonly used inducer for stress-induced premature senescence, which shares the features of replicative senescence (4). Oxidative stress-induced premature aging has been a good tool for *in vitro* aging research.

Gracilariopsis lemaneiformis, a kind of delicious seafood, is rich in active ingredients, including vitamins, polysaccharides, nicotinic acid, proteins, and dietary fiber (5). It was indicated that *G. lemaneiformis* polysaccharides (GPs) possess various biological activities, such as antitumor, antioxidant, and immune regulatory (6–11). Till present, the primary method of polysaccharide extraction is using hot water. However, there is a disadvantage of high energy consumption and long extraction time (12). Acid can effectively degrade the glycosidic bonds of polysaccharides and improve the yield of small molecular polysaccharides (13). Hydrochloric acid and citric acid are the most commonly used as medium at present.

In this study, a model *in vitro* was established that the human embryonic lung diploid cells (2BS) were treated with a sub-lethal dosage of H_2O_2 to study the protective potential of PGP against cellular senescence. Alterations in cellular morphology, senescence-associated β-galactosidase (SA-β-gal) activity, cell cycle, and molecular expression were evaluated to illustrate the possibly associated molecular mechanisms.

MATERIALS AND METHODS

Samples

G. lemaneiformis was collected from Xiapu County farm, Fujian Province. It was cleaned repeatedly and removed sediment and other sundries in the laboratory, then grounded and crushed after natural drying, and sealed for standby after 200 mesh screening.

Extraction and Purification of GP

A solution of 50 g seaweed powder in 1,000 ml distilled water was added to 0.15 g cellulose and stirred at 50°C for 3 h. Later, 25 g citric acid monohydrate was added for reaction at 95°C for 2 h. The extraction solution was filtered and centrifuged at 5,000 r/min for 15 min. The supernatant was adjusted to pH 7 with 10% ammonia and then concentrated and dialyzed. The extract solution was added to ethanol, and the precipitate was dried to obtain GP.

A solution of GP in distilled water was purified by gel chromatography on a Sephadex G-100 column (50 cm × 2.6 cm) eluted with tap water (0.2 ml/min). The fraction obtained was dialyzed and freeze-dried to yield a purified polysaccharide (PGP).

Structural Analysis

Routine component, including total sugar and sulfate content, was detected according to the previous method (14–16). Infrared spectrums were measured by a Nicolet Avatar 360 with KBr disks. Molecular weight and monosaccharide composition were determined by High Performance Gel Permeation Chromatography (HPGPC) and Gas Chromatography—Mass Spectrometry (GC-MS). ^{1}H and ^{13}C NMR spectra (e.g., 2D COSY, TOCSY, and DEPT) of samples were recorded using an AVANCE 600 MHz with a triple resonance probe.

Cell Viability Assay

2BS cells were cultured as a monolayer in Dulbeo's Modification of Eagle's Medium (DMEM) supplemented with 10% Fetal Bovine Serum (FBS) in a 37°C, 5% CO_2 humidified incubator. For drug administration, the culture medium was removed and PGP at indicated concentrations (e.g., 10, 50, 100, and 200 μg/ml) was added into each well for 2 h incubation, followed by treatment with 200 μM H_2O_2 for 1 h to induce premature senescence. Then, the H_2O_2-containing medium was replaced with a fresh medium for an additional 48 h before harvest. Cell viability was assessed by the Cell Counting Kit-8 assay, as described previously (17). Each compound was tested in triplicate and the experiments were repeated three times.

SA-β-Gal and DAPI Staining

Detection of *SA-β-Gal*-positive cells was performed, as described previously, according to the indications provided with the staining kit (18). All the experiments were repeated three times, and one of the representative results was shown. DNA was visualized by 4',6-diamidino-2-phenylindole (DAPI) (1 μg/ml) after fixation with 4.0% paraformaldehyde (PFA) (19).

Western Blot Analysis

An equal number of 2BS cells from the different groups were lysed using a sample buffer. Western blotting was performed, as described previously, according to the standard procedures. The sample was separated by 10% Sodium Dodecyl Sulfate PolyAcrylamide Gel Electrophoresis (SDS-PAGE) and transferred to nitrocellulose membranes. After being blocked in evaporated non-fat milk for 4 h, the membranes were incubated with 1% Bovine Serum Albumin (BSA) solution dissolving primary anti-bodies (p53, p21). Protein bands were visualized using horseradish peroxidase-conjugated secondary antibodies. Protein bands were quantified by densitometry and normalized to glyceraldehyde-3-phosphate dehydrogenase (GAPDH).

Statistical Analysis

All the data were presented as mean ± SD. A value of $p < 0.05$ was considered statistically significant. Differences between groups were evaluated by one-way ANOVA followed by Duncan's multiple range tests.

RESULTS

Chemistry of PGP

The soluble polysaccharide of *G. lemaneiformis* (GP) obtained by acid extraction was a non-gelling polysaccharide. Gel chromatography on dextran G100 separated the sulfated polysaccharide from GP into one peak, named PGP (**Figure 1A**). The latter was eluted as a single symmetrical peak corresponding to an average molecular weight of 2.7×10^3 Da, as determined by the high Performance Liquid Chromatography (HPLC) method. A lack of absorption at 280 nm indicated that PGP contained no protein.

The PGP contained 92.65% of total sugar and 5.37% of sulfate on the basis of fraction dry weight. Sugar compositional analysis revealed that PGP consists of polysaccharides containing a high amount of galactose together with a smaller amount of glucose unit.

Figure 1B exhibits the major functional groups and the chemical bonds of PGP. As shown, the broad absorption at 3,420 cm^{-1} was corresponded to the O–H stretching vibration,

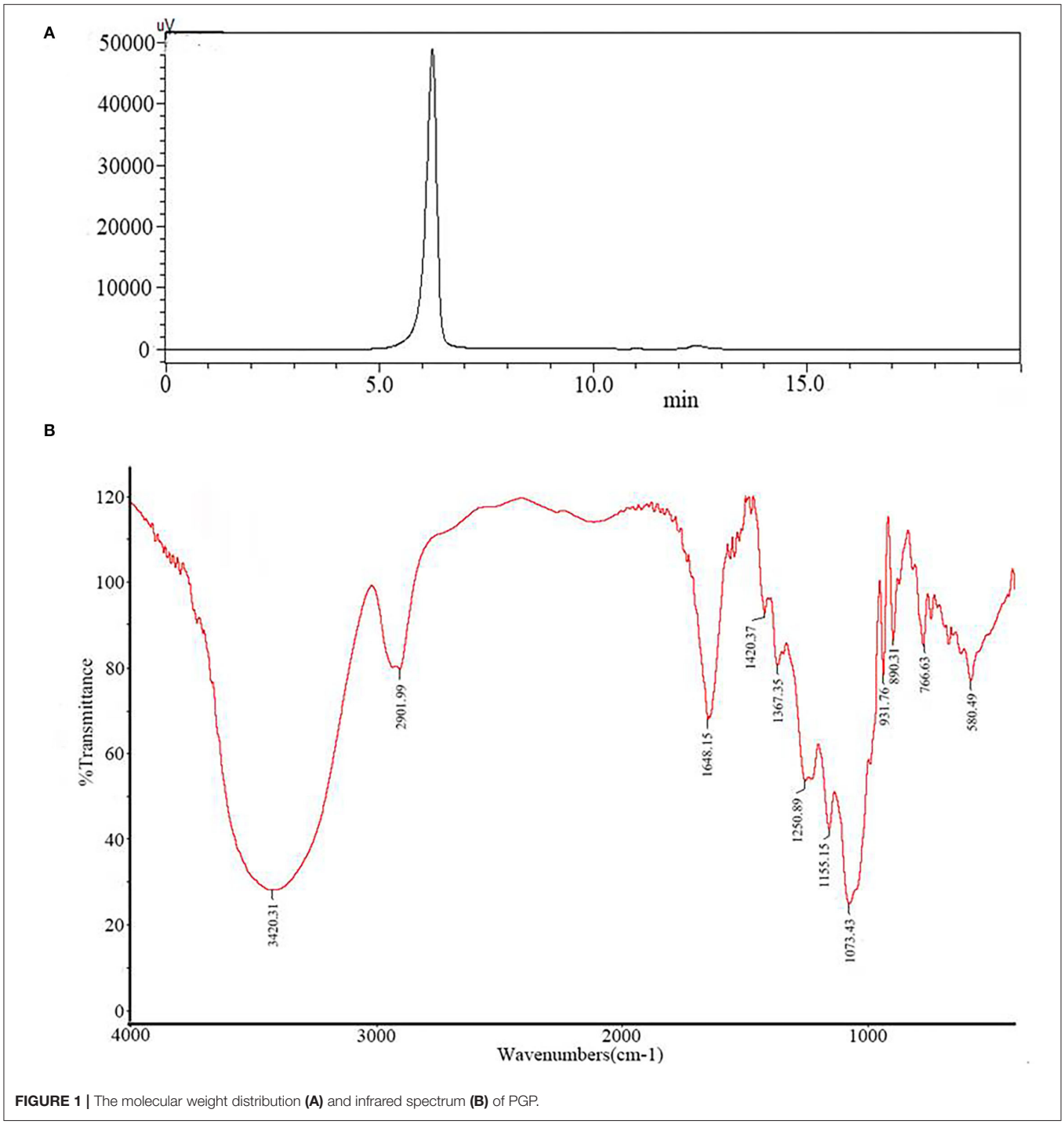

FIGURE 1 | The molecular weight distribution **(A)** and infrared spectrum **(B)** of PGP.

and the strong band at 2,902 cm^{-1} was ascribed to stretching vibrations of C–H. Two bands at 1,648 and 1,420 cm^{-1} were assigned to the absorbance of the deprotonated COO– group (20). These characteristics indicated that PGP was a typical acidic polysaccharide, which agreed with the content of uronic acid (9.84%). The bands at 1,250 and 931 cm^{-1} can be attributed to the S=O vibration of the sulfate groups and the C–O–C of 3,6-anhydro-a-L-galp (21). The peak at 820 cm^{-1} indicated that sulfate groups were located in position C6 of the galactose ring (22).

Structure of PGP

Methylation analysis of the sulfated PGP demonstrated the presence of a variety of methylated derivatives. In fact, methylation of sulfated polysaccharides does not always yield reliable proportions of methylated alditol acetates (23, 24). As shown in **Table 1**, it was probable that there was incomplete methylation. The peak type was relatively simple. The terminal group only exists in the form of Gal-(1→ indicating that galactose is the main terminal residue of PGP. The absence of other branched end residues indicated that most of the

TABLE 1 | Analysis of PGP methylation.

RT	Methylated sugar	Mass fragments (m/z)	Molar ratios	Type of linkage
17.661	2,3,4,6-Me_4-Galp	43,71,87,101,117,129,145,161,205	0.10	Gal-(1→
21.247	2,3,6-Me_3-Galp	43,87,99,101,113,117,129,131,161,173,233	0.34	→ 4)-Galp-(1→
21.549	2,4,6-Me_3-Galp	43,71,85,87,99,101,117,129,161	0.42	→ 3)-Galp-(1→
22.362	2,4-Me_2-Galp	43,71,87,99,101,117,129,139,159,173,189	0.14	→ 3,6)-Galp-(1→

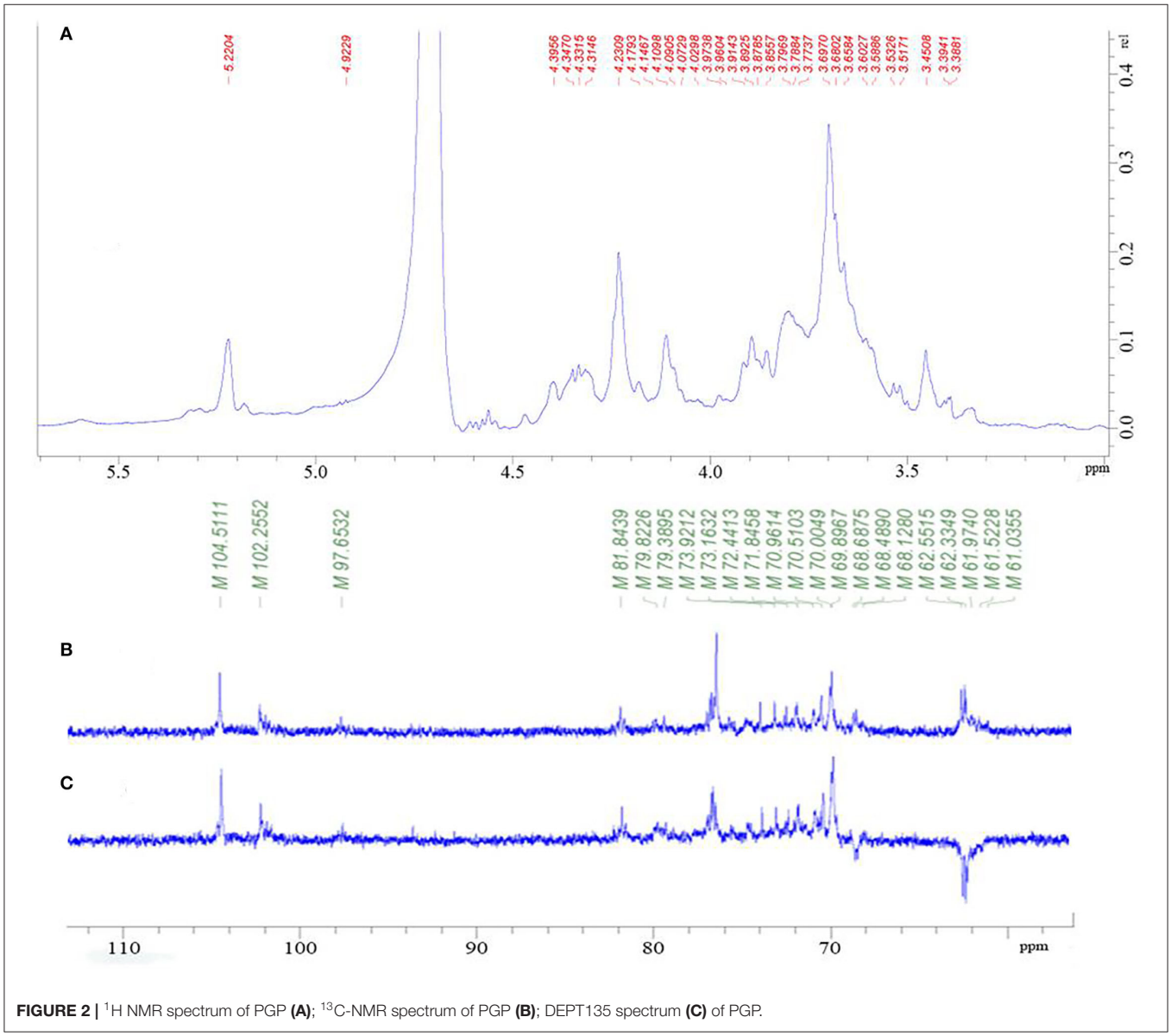

FIGURE 2 | ^{1}H NMR spectrum of PGP **(A)**; ^{13}C-NMR spectrum of PGP **(B)**; DEPT135 spectrum **(C)** of PGP.

branched chains may be degraded by citric acid. The proportion of 1→ 3 Gal and 1→ 4 Gal was similar, indicating that there was a common disaccharide unit in red algae. → 3,6)-Galp-(1→ indicated that there were substituted sulfate and galactose residues at C-6.

The NMR analysis was employed to determine the saccharide backbone structure and also to determine the sulfation pattern of the sulfated galactan. From **Figure 2A**, the proton signal of the sugar ring is mainly concentrated in δ 3.2–4.0. Furthermore, the signal peaks of end group proton (δ 5.22, 4.92, 4.40, and 4.35) were concentrated in the area of δ 4.3–5.5. The signals from an anomeric proton at δ 5.15 and 5.22 were assigned to 3,6-α-L-anhydrogalactose (LA) and α-L-galactose-6-sulfate (L-6S), respectively. However, it was obvious that the signal of δ

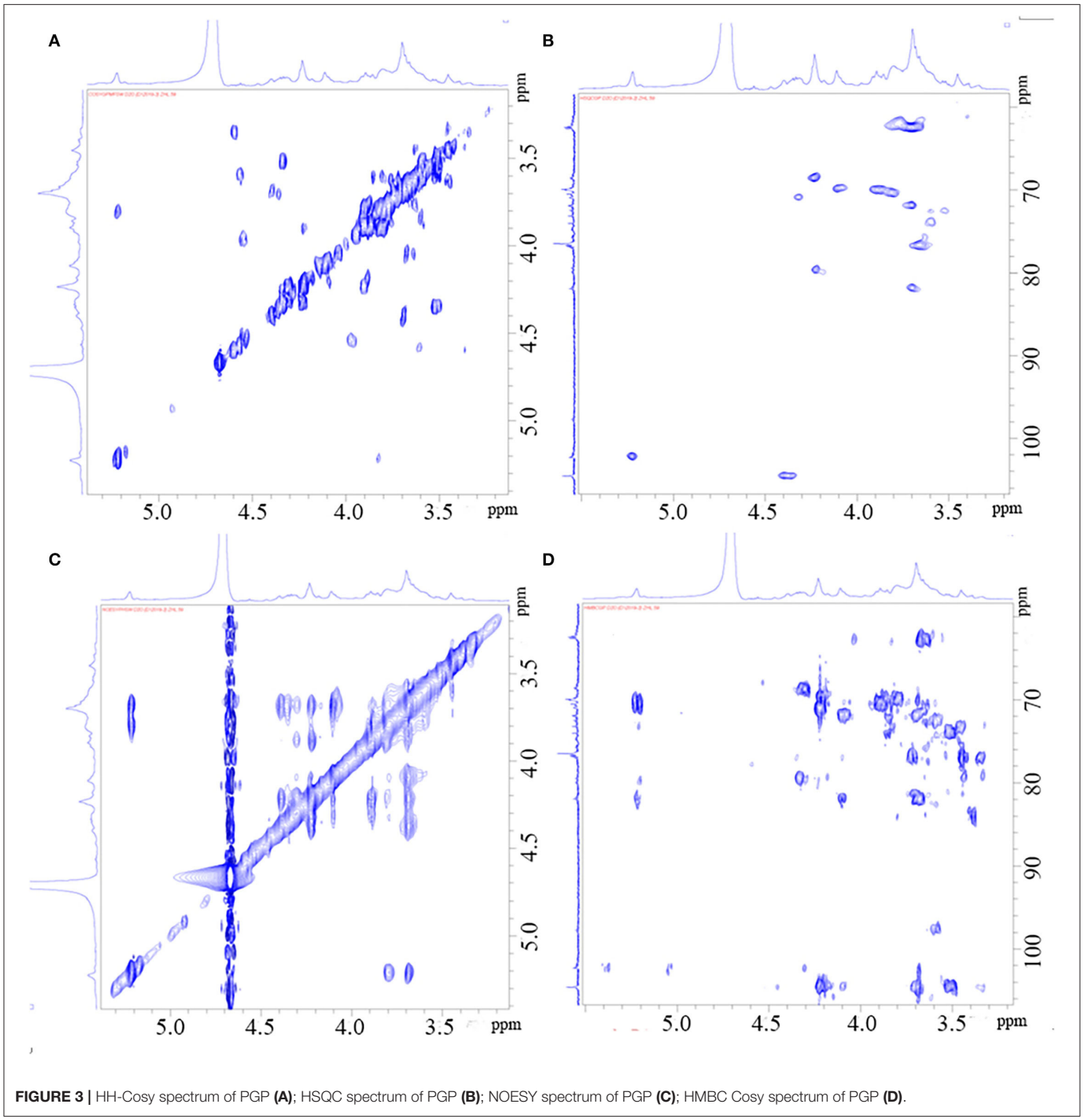

FIGURE 3 | HH-Cosy spectrum of PGP **(A)**; HSQC spectrum of PGP **(B)**; NOESY spectrum of PGP **(C)**; HMBC Cosy spectrum of PGP **(D)**.

5.22 was much greater than δ 5.15, indicating the C-6 position of (1→ 4)-α-L-galactose was mainly substituted by the sulfate group but not LA.

As shown in **Figure 2**, there were several main anomeric carbon signal peaks (δ 104.51, 102.26, and 97.65) of NMR carbon spectrum signal mainly located in δ 93–105. Among them, δ 104.51 and 102.26 were mainly β isomeric carbon, and δ 97.65 was mainly α isomeric carbon and β reductive terminal heterocarbon signal. The strong signal δ 70 also showed the existence of 6-OSO_3-α-L-galactose. Dept135 spectrum showed that δ 68.66, 62.54, 62.37, and 62.28 were inverted peaks, indicating the chemical shift of C6, and the peak at δ 68.66 migrates to the low field, indicating the substitution of C6.

Through the HSQC spectrum, it could be observed that δ 102.4 was the heterocephalic carbon signal. The corresponding heterocephalic hydrogen signal in HSQC spectrum was δ 5.22. We could infer that H1–H5 were, respectively, δ 5.22, 3.80,

TABLE 2 | Glycosidic bond signal attribution of PGP.

Glycosyl residues	H1 C1	H2 C2	H3 C3	H4 C4	H5 C5	H6a C6	H6b
→ 4)-α-D-Galp-(1→	5.22	3.8	3.9	4.23	4.32	3.68	ns
	102.4	70.45	70.05	79.55	70.93	62.44	
→ 3)-β-D-Galp-(1→	4.4	3.68	3.7	4.1	3.65	4.21	ns
	104.56	71.89	81.89	69.85	76.55	68.55	
→ 3,6)-β-D-Galp-(1→	4.4	3.68	3.7	4.1	3.65	4.21	ns
	104.56	71.89	81.89	69.85	76.55	68.55	
α-D-Galp-(1→	5.21	3.95	3.51	3.6	3.45	3.65	ns
	102.9	70.26	72.35	72.6	74.5	62.19	

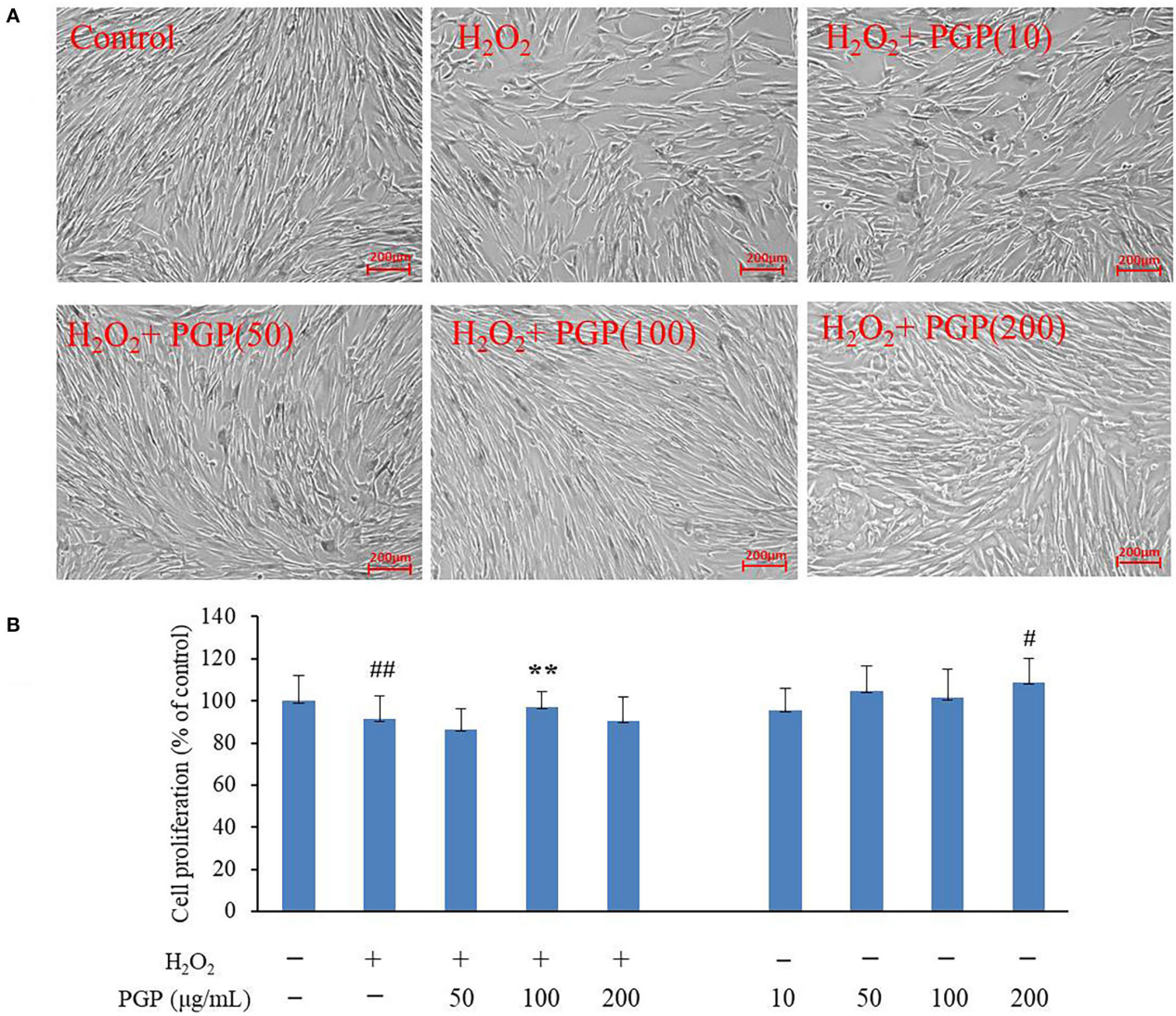

FIGURE 4 | The effect of PGP on cell morphology **(A)** and cell viability in H_2O_2-treated young 2BS cells at PD28 **(B)** (**$p < 0.01$ vs. H_2O_2 alone group; ##$p < 0.01$ vs. control group). Young 2BS cells at PD28 were incubated with 200 μM H_2O_2 at 37°C in the culture medium for 2 h. Then, H_2O_2-containing medium was replaced with fresh medium containing 10, 50, 100, and 200 μg/ml of PGP for additional 72 h before being morphologically observed at the magnification of 10×. Figures are representative of three independent experiments. #$p < 0.05$ vs. control group.

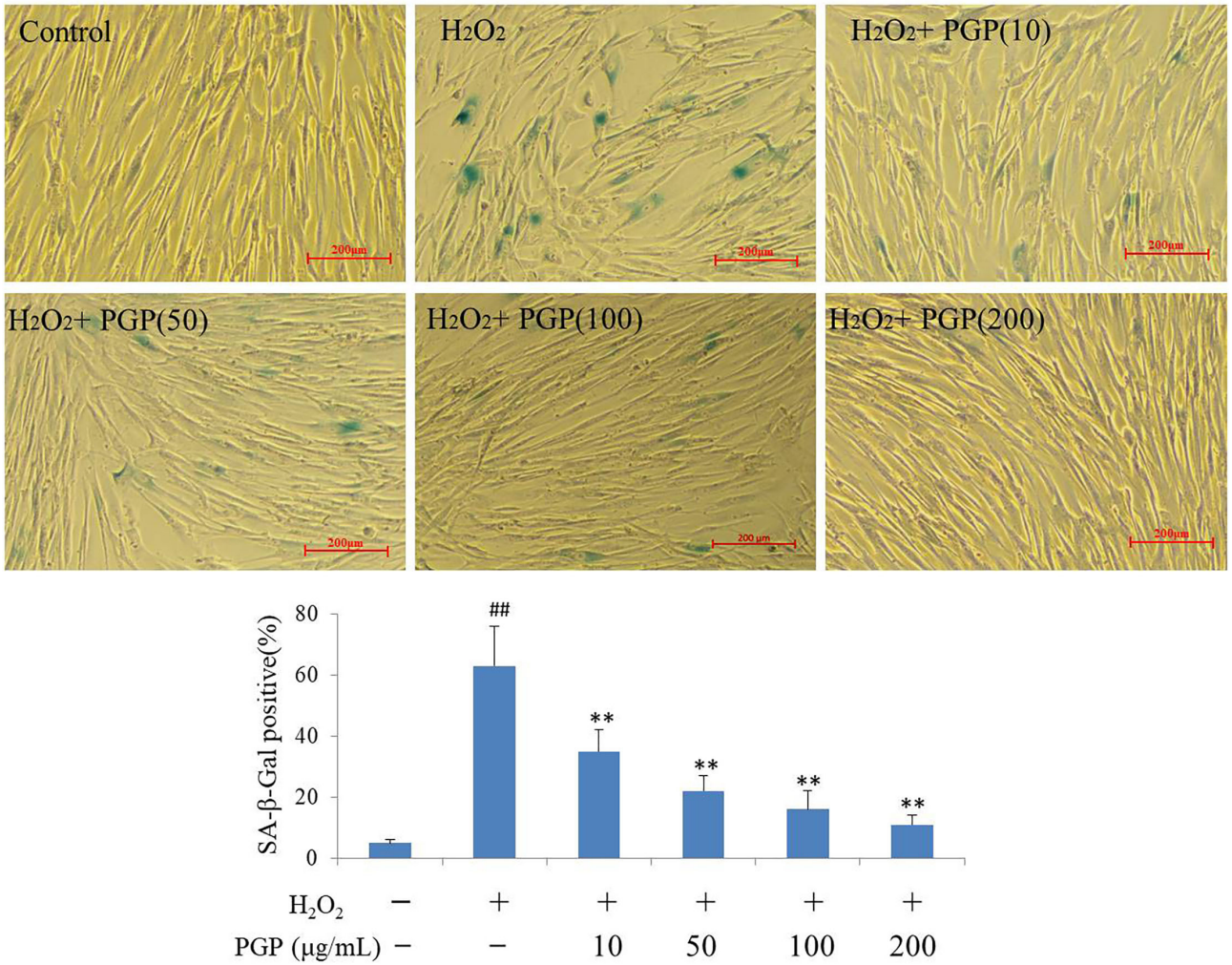

FIGURE 5 | The SA-β-Gal staining of young 2BS cells treated with H_2O_2 followed by PGP (**$p < 0.01$ vs. H_2O_2 alone group; ##$p < 0.01$ vs. control group). PD28 2BS cells were seeded in 24-well plates for 20 h before quick exposure to H_2O_2 as stated above. The cells were then incubated in fresh medium without or with PGP for additional 5 days. Cells were photographed at the magnification of 10×. The percentage of SA-β-gal-positive cells out of the total cells was counted and the average data were obtained from three independent experiments.

3.90, 4.23, 4.32, and 3.68. The corresponding C1–C5 is δ 102.40, 70.45, 70.05, 79.55, and 70.93. Therefore, the signal should be attributed to the glycosidic bond → 4)-α-Galp-(1→ . In the HMBC spectrum (**Figure 3**), we assigned the glycosidic bond signals of polysaccharides according to the one-dimensional and two-dimensional NMR spectrum. The isomeric hydrogen of → 4)-α-D-Galp has a correlation signal peak with its own C4, indicating the presence of → 4)-α-D-Galp-(1→ 4)-α-D-Galp-(1→ link mode. The isomeric hydrogen of → 3,6)-β-D-Galp-(1→ and H3 of → 3)-β-D-Galp-(1→ has a relevant signal peak, indicating the presence of → 3,6)-β-D-Galp-(1→ 3)-β-D-Galp-(1→ 3)-β-D-Galp-(1→ . The isomeric carbon of → 3)-β-D-Galp-(1→ and H4 of → 4)-α-D-Galp-(1→ has a relevant signal peak, indicating the presence of → 3)-β-D-Galp-(1→ 4)-α-D-Galp-(1→ . We combined the HMBC and NOESY spectra to assign all glycosidic bond signals, as shown in **Table 2**.

From the above results, it could be seen that PGP is a linear polysaccharide containing alternating α-(1→ 3)- and β-(1→ 4)-galactopyranose units. Most of the sulfate groups are at C6 of the -(1→ 4)-α-D-Galp, and a small part of them are etherified at C3 and C6. The methoxy signal of each type of sugar was weak, indicating that some residues were methylated. The fine structure needs to be further analyzed.

Cell Morphology and Viability

The MTT assay was performed to test the possible cytotoxic effects of different concentrations of PGP on cell growth. The results showed that an apparent reduction of cell proliferation was not observed upon drug treatment until the dose reached 200 μg/ml (**Figure 4**). It could be seen that normal young 2BS cells grow in a spindle shape and arrange regularly. They had vigorous vitality, more division phases, and clear cell boundaries. Instead, the activity of 2BS cells in the H_2O_2

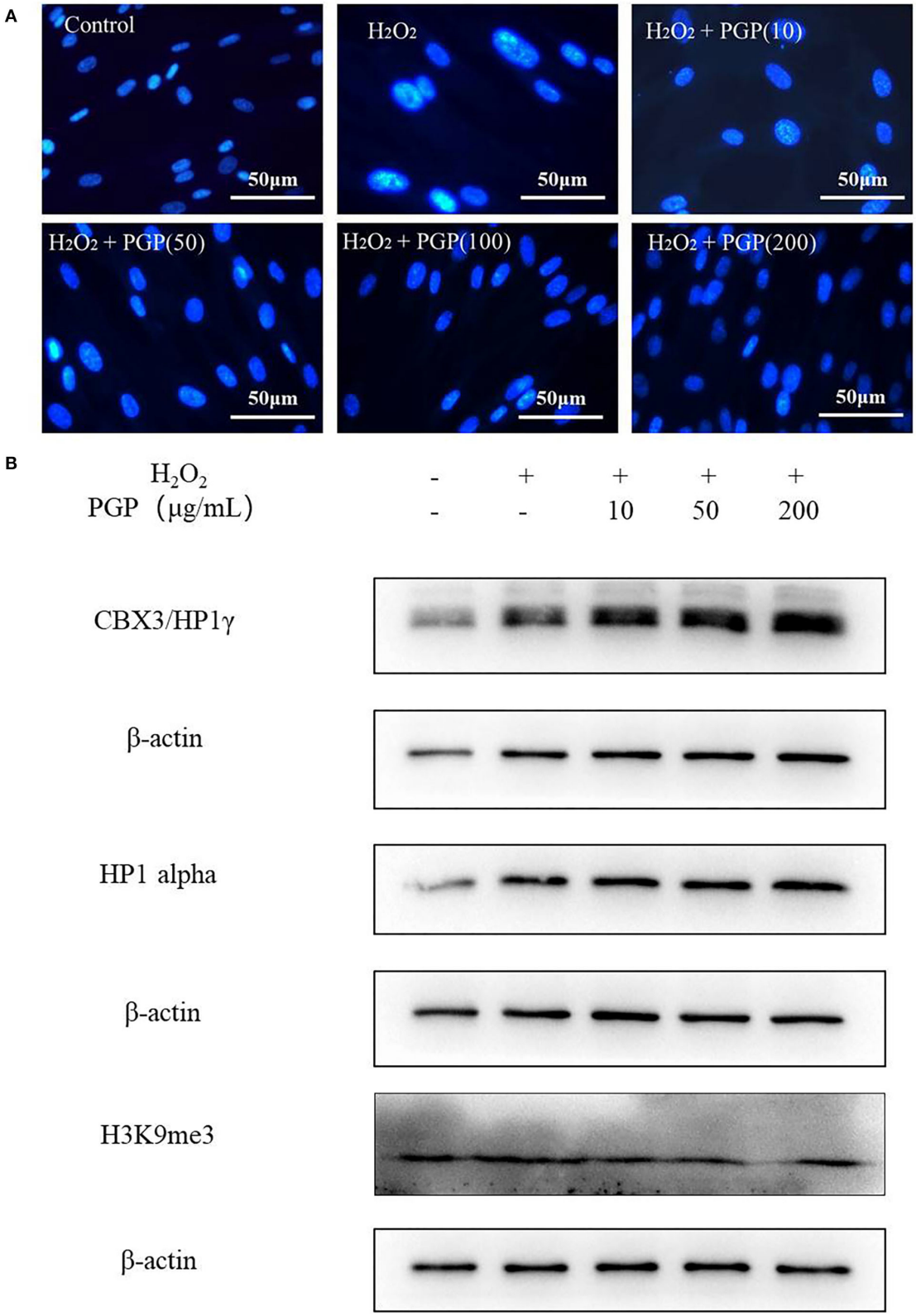

FIGURE 6 | Senescence-associated heterochromatic foci (SAHF) formation **(A)** and the expression levels of three proteins (HP1a, HP1g, and H3k9me3) **(B)** in the nucleus of senescent 2BS cells visualized by DAPI staining. Permeabilize the cells by incubating the coverslips in 0.2% (v/v) Triton-X 100 in PBS (pH 7.3) for 5 min at room temperature. Stain SAHF by incubating the coverslips with 0.15 μg/ml final concentration of DAPI diluted in 3% (w/v) BSA in PBS, pH 7.3 for 3 min. After the slides have dried, observe SAHF using a fluorescent microscope.

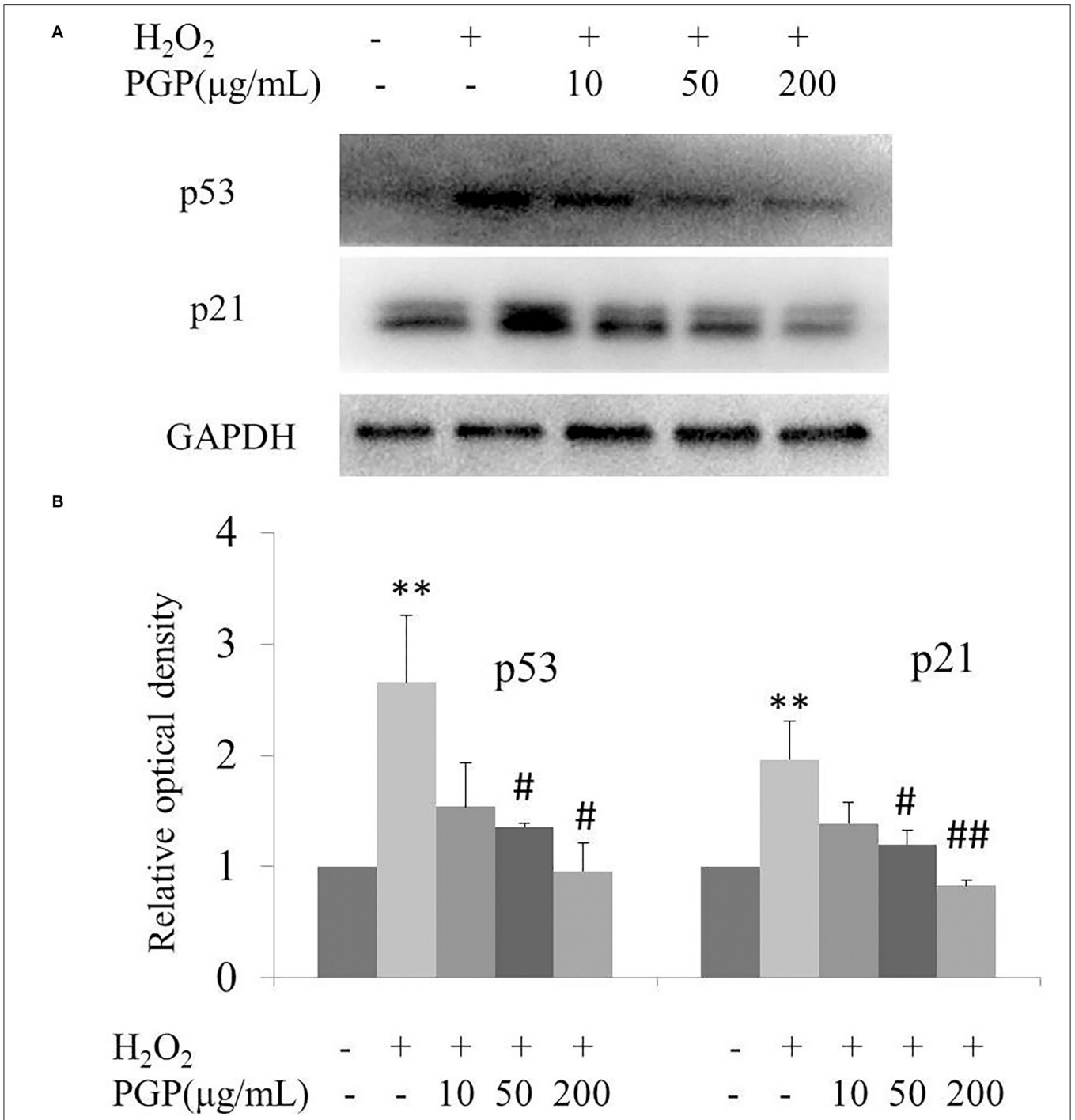

FIGURE 7 | The expression of senescence-associated proteins **(A)** and relative optical density of P53 and P21 in H_2O_2-treated young 2BS cells incubated with various concentrations of PGP (**$p < 0.01$ vs. control group; #$p < 0.05$ vs. H_2O_2 alone group; ##$p < 0.01$ vs. H_2O_2 alone group). Bars represent relative protein levels counted as *D*1/*D*0 (the value for control was set as 1.0), where *D*0 and *D*1 stand for the optical density of GAPDH ladder and sample ladder, respectively. The optical density for each ladder was calculated using the ImageJ software. Data were obtained from three independent experiments.

treatment group is significantly decreased about 20%. The growth of cells is stagnant. The cell body becomes larger and the shape is flat. The arrangement is irregular, which was similar to replicative aging cells. The cytoplasmic area becomes larger, more particles or vacuoles can be seen in the cytoplasm, and the boundary is fuzzy (4). After the administration of PGP, the cells showed faint senescent morphology characteristics and displayed a fusiform appearance with oval nuclei, which could

improve the cell senescence caused by H_2O_2 treatment in a dose-dependent manner. It was found that an exposure of 2BS cells to PGP (100 μg/ml) caused a significant livability increase of ∼16% ($p < 0.01$).

SA-β-Gal Activity

The SA-β-gal stain is widely used to detect the signal of cellular senescence. The assay utilizes a fluorimetric substrate and cell-derived extract samples to determine quantitatively the enzymatic activity (25). As shown in **Figure 5**, the cells would be dyed blue-green in the process of cell replicative aging. At this time, SA-β-gal-positive rate increased gradually. The Young cells showed the lighter SA-β-Gal staining, and slender fibrous cells accounted for the vast majority. Cells in H_2O_2 treatment groups showed the deep SA-β-Gal staining, the increased cell volume, and the irregular shape. The SA-β-Gal-positive cells were significantly lower in cells supplemented with PGP at the concentration of 200 μg/ml (11.7%), compared to cells cultured with H_2O_2 (63.3%) ($p < 0.01$).

DAPI Staining

At the chromatin level, the occurrence of cell senescence is often accompanied by extensive changes in chromatin structure, with dot-like aggregation of heterochromatin structure and inhibition of the expression of cell proliferation-related genes. This characteristic phenomenon is called senescence-associated heterochromatic foci (SAHF) (26). Due to the consistent localization of HP1, H3K9me2/3, and SAHF, they have become the marker proteins of aging-related heterochromatin aggregation. This provides a method for researchers to judge whether cells have entered the aging state, that is, to observe the distribution of HP1 (or H3K9me2/3) and chromatin in the nucleus at the same time by the immunofluorescence method (27). From **Figure 6**, after DAPI staining, the cells in the H_2O_2 treatment group showed an obvious aging state with enlarged nucleoli compared with the control group. This indicated that the cells had entered the aging state. PGP pretreatment could prevent the formation of SAHF induced by H_2O_2 in a dose-dependent manner. When the doses were increased to 100 and 200 μg/ml, SAHF was significantly reduced to the level close to the control group. Western blotting showed that the expression levels of three proteins (i.e., HP1α, HP1γ, and H3k9me3) were upregulated in the model group. The sample PGP could downregulated the marker protein. These results clearly indicated that PGP was able to influence the cell cycle, leading to improved cell proliferation and delaying premature senescence induced by H_2O_2.

The Expression of Senescence-Associated Molecular Markers

The results of this experiment showed that the intracellular p53 and p21 of 2BS at the protein level were significantly increased after H_2O_2 treatment. PGP could decrease the expression of p53 and p21 in a dose-dependent manner, of which the most significant downregulated levels of p53 and p21 were treated with the concentration of 200 μg/ml (**Figure 7**). It was speculated that PGP may delay aging by downregulating the expression of p21 and p53.

DISCUSSION

Acid extraction is performed to obtain polysaccharides with dilute hydrochloric acid or rare organic acid as solvent. The activity was better, and the yield of polysaccharides is in high quantity (28). However, the glycosidic bond is easy to break under acidic conditions, which will affect the activity and structure of polysaccharides, but some novel polysaccharide chains can be obtained to increase the diversity of polysaccharide structure. The outer epidermis of *G. lemaneiformis* is hard which is difficult to obtain a higher yield of polysaccharides. Therefore, searching for ways to be more efficient to extract polysaccharides had become the investigations of many researchers. At present, solvent (e.g., water) extraction, physical-assisted (ultrasonic, microwave, etc.) extraction, and enzymatic hydrolysis extraction had become the main extraction methods of GP (29). There were many related reports before, but there was a less in-depth exploration of structural analysis. The polysaccharide obtained by *G. lemaneiformis* with citric acid at a lower concentration had been reported, which had a high molecular weight (30). In our study, the concentration of citric acid was increased to obtain polysaccharides with lower molecular weight. From the results, the expected polysaccharide with lower molecular weight was obtained. After separation and purification, we obtained the polysaccharide with good water solubility. The isolation of this sulfated polysaccharide from *G. lemaneiformis* added a new type of polysaccharide to this group of red seaweeds.

Senescent cells have become an emerging target for the disease of aging (31). H_2O_2 was known to induce cellular senescence showing multiple changes. Based on this study, we have employed low-passage cells and the appropriate H_2O_2 concentration to induce premature senescence was determined to be 200 mM. Senescent cells acquire a typical flat and enlarged shape and show the increased levels of a group of senescence biomarkers, including SA-β-Gal activity, and the protein abundance of p21 and p53 (32, 33). Studies suggested that the long-term supplementation of SHQA also notably delayed the growth arrest and lessened the raise of senescence biomarkers, including p53, p21, and SA-β-Gal. Consistently, we observed that upon exposure to low-dose H_2O_2, the abundance of SA-β-Gal-positive cells was elevated in 2BS; meanwhile, the pretreatment of PGP significantly suppressed their elevations, which suggested the ability of PGP to repress the oxidative stress-induced senescence in 2BS.

The p53-p21 pathway is a relatively recognized aging-related signal pathway. Inactivation of p53 or p21 gene can prolong the replicative life of cells, indicating that this signal pathway is closely related to cell aging (34). p53 and p21 are cell cycle regulators directly related to aging (35). When cells encounter some external stimuli, it is found that the expression of p53 will be rapidly upregulated with stress, so as to further activate p21, inhibit the phosphorylation of p21 protein, block the normal

cell cycle, and then lead to cell aging. The target molecule of p53 is p21, which is a cyclin-dependent protein kinase inhibitor that inhibits cell cycle and can make cells enter an irreversible growth arrest state (36). In this study, the partial inhibitory effects of PGP on 2BS may be due to the contribution of the p53-p21 pathway.

CONCLUSION

The polysaccharides isolated from *G. lemaneiformis* were slightly methylated agarans, with a low 3,6-anhydrogalactose content, bearing sulfated mainly at the 6-position of (1→ 4)-α-D-Galp. Our studies demonstrated that H_2O_2 caused cell cycle arrest accounting for inhibition of cell proliferation, resulting in SA-β-gal activity elevation and SAHF formation. Pretreatment with PGP protected against H_2O_2-induced cellular senescence. The anti-aging effect of PGP may be involved in potentiating the p53-p21 pathway. These results suggested the promising role of PGP as an attractive food with the potential to retard senescence and senescence-related diseases.

DATA AVAILABILITY STATEMENT

The original contributions presented in the study are included in the article/supplementary material, further inquiries can be directed to the corresponding author/s.

AUTHOR CONTRIBUTIONS

XW: visualization, investigation, and validation. XX and GM: feeding cells and supporting partial data. GW and XS: methodology, data analysis, drawing charts, and writing—original and editing. YG: conceptualization, methodology, and writing —review. NX: investigation and formal analysis. ZZ: funding acquisition and supervision. All authors have read and agreed to the publishing of the current version of the manuscript.

FUNDING

This study was supported by the Zhejiang Province Basic public welfare research project (LGN21D060001) and the National Natural Science Foundation of China (31700307 and 81771520).

REFERENCES

1. Hernandez-Segura A, Nehme J, Demaria M. Hallmarks of cellular senescence. *Trends Cell Biol.* (2018) 28:436–53. doi: 10.1016/j.tcb.2018.02.001
2. Tokmakov AA, Sato KI. Activity and intracellular localization of senescence-associated β-galactosidase in aging Xenopus oocytes and eggs. *Exp Gerontol.* (2019) 119:157–67. doi: 10.1016/j.exger.2019.02.002
3. Wang Y, Gao JJ, Wu F, Lai CY, Li YQ, Zhang GQ, et al. Biological and epigenetic alterations of mitochondria involved in cellular replicative and hydrogen peroxide-induced premature senescence of human embryonic lung fibroblasts. *Ecotoxicol Environ Saf.* (2021) 216:112204. doi: 10.1016/j.ecoenv.2021.112204
4. Toussaint O, Medrano EE, Zglinicki T. Cellular and molecular mechanisms of stress-induced premature senescence (SIPS) of human diploid fibroblasts and melanocytes. *Exp Gerontol.* (2000) 35:927–45. doi: 10.1016/S0531-5565(00)00180-7
5. Luo HT, Wang Q, Zhang CW, Zhang L, Yang YF. Bioaccumulation and release of heavy metals during growth and decomposition of cultivated *Gracilaria lemaneiformis*. *Mar Pollut Bull.* (2021) 173:113130. doi: 10.1016/j.marpolbul.2021.113130
6. Jiang WT, Fu YT, Yang F, Yang YF, Liu T, Zheng WJ, et al. *Gracilaria lemaneiformis* polysaccharide as integrin-targeting surface decorator of selenium nanoparticles to achieve enhanced anticancer efficacy. *ACS Appl Mater Inter.* (2014) 6:13738–48. doi: 10.1021/am5031962
7. Kang YN, Wang ZJ, Xie DS, Sun X, Yang WG, Zhao XD, et al. Characterization and potential antitumor activity of polysaccharide from *Gracilariopsis lemaneiformis*. *Mar Drugs.* (2017) 15:100–13. doi: 10.3390/md15040100
8. Liao XB, Yang LW, Chen MZ, Yu J, Zhang SM, Ju YY. The hypoglycemic effect of a polysaccharide (glp) from *Gracilaria lemaneiformis* and its degradation products in diabetic mice. *Food Funct.* (2015) 6:2542–49. doi: 10.1039/C4FO01185F
9. Liu QM, Yang Y, Maleki SJ, Alcocer MJC, Xu SS, Shi CL. Anti-food allergic activity of sulfated polysaccharide from *Gracilaria lemaneiformis* is dependent on immunosuppression and inhibition of p38 mapk. *J Agric Food Chem.* (2016) 64:4536–44. doi: 10.1021/acs.jafc.6b01086
10. Wen LR, Zhang YL, Sunwaterhouse DX, You LJ, Fu, X. Advantages of the polysaccharides from *Gracilaria lemaneiformis* over metformin in antidiabetic effects on streptozotocin-induced diabetic mice. *RSC Adv.* (2017) 7:9141–51. doi: 10.1039/C6RA26970B
11. Xu JT, Gao KS. Growth, pigments, UV-absorbing compounds and agar yield of the economic red seaweed *Gracilaria lemaneiformis* (Rhodophyta) grown at different depths in the coastal waters of the South China Sea. *J Appl Phycol.* (2007) 20:231–36. doi: 10.1007/978-1-4020-9619-8_29
12. Qiu SM, Aweya JJ, Liu XJ, Liu Y, Tang SJ, Zhang WC, et al. Bioactive polysaccharides from red seaweed as potent food supplements: a systematic review of their extraction, purification, and biological activities. *Carbohydr Polym.* (2022) 275:118696. doi: 10.1016/j.carbpol.2021.118696
13. Trygg J, Beltrame G, Yang BR. Rupturing fungal cell walls for higher yield of polysaccharides: acid treatment of the basidiomycete prior to extraction. *Innov Food Sci Emerg Technol.* (2019) 57:102206. doi: 10.1016/j.ifset.2019.102206
14. Jain VM, Karibasappa GN, Dodamani AS, Mali GV. Estimating the carbohydrate content of various forms of tobacco by phenol-sulfuric acid method. *J Educ Health Promot.* (2017) 6:90–95. doi: 10.4103/jehp.jehp_41_17
15. He YL, Ye M, Jing LY, Du ZZ, Surahio M, Xu HM. Preparation, characterization and bioactivities of derivatives of an exopolysaccharide from *Lachnum*. *Carbohydr Polym.* (2015) 117:788–96. doi: 10.1016/j.carbpol.2014.10.046
16. Yaphe W, Arsenault GP. Improved resorcinol reagent for the determination of fructose, and of 3,6-anhydrogalactose in polysaccharides. *Anal Biochem.* (1965) 13:143–48. doi: 10.1016/0003-2697(65)90128-4
17. Zhang ZS, Wang XM, Su HL, Pan YL, Han JF, Zhang TS, et al. Effect of sulfated galactan from *Porphyra haitanensis* on H_2O_2-induced premature senescence in WI38 cells. *Int J Biol Macromol.* (2018) 106:1235–39. doi: 10.1016/j.ijbiomac.2017.08.123
18. Huang TT, Rivera-Pérez JA. Senescence-associated β-galactosidase activity marks the visceral endoderm of mouse embryos but is not indicative of senescence. *Genesis.* (2014) 52:300–308. doi: 10.1002/dvg.22761
19. Schmid I, Uittenbogaart C, Jamieson BD. Live-cell assay for detection of apoptosis by dual-laser flow cytometry using Hoechst 33342 and 7-amino-actinomycin D. *Nat Prot.* (2007) 2:187–90. doi: 10.1038/nprot.2006.458
20. Manrique GD, Lajolo FM. FT-IR spectroscopy as a tool for measuring degree of methyl esterification in pectins isolated from ripening papaya fruit. *Postharvest Biol Technol.* (2002) 25:99–107. doi: 10.1016/S0925-5214(01)00160-0
21. Yamaguchi T, Takamura H, Matoba T, Terao J. Antioxidative activity of heterocyclic compounds found in coffee volatiles produced by Maillard reaction. *J Agric Food Chem.* (2002) 50:5480–84. doi: 10.1021/jf025616h

22. Maciel JS, Chaves LS, Souza BWS, Teixeira DIA, Freitas ALP, Feitosa JPA, et al. Structural characterization of cold extracted fraction of soluble sulfated polysaccharide from red seaweed *Gracilaria birdiae*. *Carbohydr Polym.* (2008) 71:559–65. doi: 10.1016/j.carbpol.2007.06.026
23. Patankar MS, Oehninger S, Barnett T, Williams RL, Clark GF. A revised structure for fucoidan may explain some of its biological activities. *J Biol Chem.* (1993) 268:21770–76. doi: 10.1016/S0021-9258(20)80609-7
24. Pereira MS, Mulloy B, Mourao PAS. Structure and anticoagulant activity of sulfated fucans. *J Biol Chem.* (1999) 274:7656–67. doi: 10.1074/jbc.274.12.7656
25. Ravelojaona V, Robert AM, Robert L. Expression of senescence- associated β-galactosidase (SA-β-Gal) by human skin fibroblasts, effect of advanced glycation end-products and fucose or rhamnose-rich polysaccharides. *Arch Gerontol Geriatr.* (2009) 48:151–54. doi: 10.1016/j.archger.2007.12.004
26. Narita M, Nuñez S, Heard E, Narita M, Lin AW, Hearn SA, et al. Rb-mediated heterochromatin formation and silencing of E2F target genes during cellular senescence. *Cell.* (2003) 113:703–16. doi: 10.1016/S0092-8674(03)00401-X
27. Funayama R, Saito, Tanobe H, Ishikawa F. Loss of linker histone H1 in cellular senescence. *J. Cell Biol.* (2006) 175:869–80. doi: 10.1083/jcb.200604005
28. Li X, Xie QT, Huang SM, Shao P, You LJ, Pedisic S. Digestion & fermentation characteristics of sulfated polysaccharides from *Gracilaria chouae* using two extraction methods *in vitro* and *in vivo*. *Food Res Int.* (2021) 145:110406. doi: 10.1016/j.foodres.2021.110406
29. Long XS, Hu X, Liu SC, Pan C, Chen SJ, Li LH, et al. Insights on preparation, structure and activities of *Gracilaria lemaneiformis* polysaccharide. *Food Chem.* (2021) 12:100153. doi: 10.1016/j.fochx.2021.100153
30. Ren YL, Zheng GQ, You LJ, Wen LR, Li C, Fu X, et al. Structural characterization and macrophage immunomodulatory activity of a polysaccharide isolated from *Gracilaria lemaneiformis*. *J Funct Foods.* (2017) 33:286–96. doi: 10.1016/j.jff.2017.03.062
31. Gruber HE, Ingram JA, Davis DE, Hanley EN. Increased cell senescence is associated with decreased cell proliferation *in vivo* in the degenerating human annulus. *Spine J.* (2009) 9:210–15. doi: 10.1016/j.spinee.2008.01.012
32. Veroutis D, Kouroumalis A, Lagopati N, Polyzou A, Chamilos C, Papadodima S, et al. Evaluation of senescent cells in intervertebral discs by lipofuscin staining. *Mech Ageing Dev.* (2021) 199:111564. doi: 10.1016/j.mad.2021.111564
33. Ben-Porath I, Weinberg RA. The signals and pathways activating cellular senescence. *Int J Biochem Cell Biol.* (2005) 37:961–76. doi: 10.1016/j.biocel.2004.10.013
34. Jin H, Lian N, Zhang F, Chen L, Chen Q, Lu C, et al. Activation of PPARγ/P53 signaling is required for curcumin to induce hepatic stellate cell senescence. *Cell Death Dis.* (2016) 7:e2189–99. doi: 10.1038/cddis.2016.92
35. Yang JF, Lu YC, Yang PP, Chen QF, Wang Y, Ding Q, et al. MicroRNA-145 induces the senescence of activated hepatic stellate cells through the activation of p53 pathway by ZEB2. *J Cell Physiol.* (2019) 234:7587–99. doi: 10.1002/jcp.27521
36. Zhang RG, Chen W, Adams PD. Molecular dissection of formation of senescence-associated heterochromatin foci. *Mol Cell Biol.* (2007) 27:2343–58. doi: 10.1128/MCB.02019-06

Conflict of Interest: The authors declare that the research was conducted in the absence of any commercial or financial relationships that could be construed as a potential conflict of interest.

Publisher's Note: All claims expressed in this article are solely those of the authors and do not necessarily represent those of their affiliated organizations, or those of the publisher, the editors and the reviewers. Any product that may be evaluated in this article, or claim that may be made by its manufacturer, is not guaranteed or endorsed by the publisher.

Copyright © 2022 Wang, Xu, Mao, Guo, Wang, Sun, Xu and Zhang. This is an open-access article distributed under the terms of the Creative Commons Attribution License (CC BY). The use, distribution or reproduction in other forums is permitted, provided the original author(s) and the copyright owner(s) are credited and that the original publication in this journal is cited, in accordance with accepted academic practice. No use, distribution or reproduction is permitted which does not comply with these terms.